HEARING AID-COMPATIBLE INTERNAL LTE/WWAN BAR-TYPE MOBILE PHONE ANTENNA

Shu-Chuan Chen and Kin-Lu Wong
Department of Electrical Engineering, National Sun Yat-sen University, Kaohsiung 80424, Taiwan; Corresponding author: chensc@ema.ee.nsysu.edu.tw

Received 23 June 2010

ABSTRACT: *An internal eight-band LTE/WWAN on-board printed antenna meeting the hearing air compatibility (HAC) specification of ANSI C63.19-2007 in the bar-type mobile phone is presented. The antenna is a coupled-fed inverted-F antenna directly printed on the system circuit board of the mobile phone and can generate two wide operating bands (698–960/1710–2690 MHz) to respectively cover the LTE700/ GSM850/900 and GSM1800/1900/UMTS/LTE2300/2500 operation. With the antenna disposed on the bottom edge of the circuit board and surrounded by an L-shape ground plane, the near-field strengths of the emitted electric and magnetic fields 15 mm above the acoustic output are evaluated to be in category M3 or M4 of the HAC specification. That is, the mobile phone with the embedded LTE/WWAN antenna can be treated as a hearing aid-compatible wireless device. Details of the HAC results are presented. Effects of the user's hand holding the mobile phone on the near-field emission of the antenna are also analyzed.* © 2011 Wiley Periodicals, Inc. Microwave Opt Technol Lett 53:774–781, 2011; View this article online at wileyonlinelibrary.com. DOI 10.1002/mop.25837

Key words: *mobile antennas; internal mobile phone antennas; on-board printed antennas; HAC mobile phones*

1. INTRODUCTION

The hearing aid compatibility (HAC) specification of ANSI C63.19-2007 [1] requires that at least half of all mobile phones on the U.S. market must have RF interference level of category M3 or M4 of ANSI C63.19-2007 [1]. The RF interference level of the mobile phone is determined from the near-field strengths of the emitted electric and magnetic fields of the embedded antenna on the observation plane centered above 15 mm of the acoustic output. For example, based on ANSI C63.19-2007 [1], for frequencies below 960 MHz, the near-field strengths of the electric and magnetic fields must be lower than 48.5 dBV/m and −1.9 dBA/m, respectively, for the GSM850/900 operation (824–894/880–960 MHz) to be rated at least in category M3. For the LTE700 operation (698–787 MHz), the corresponding near-field strengths of the electric and magnetic fields must be lower than 51.0 dBV/m and 0.6 dBA/m, respectively.

While for frequencies above 960 MHz, the near-field strengths of the electric and magnetic fields must be lower than 38.5 dBV/m and −11.9 dBA/m, respectively, for the GSM1800/1900 (1710–1880/1850–1990 MHz) operation to be rated at least in category M3. For the UMTS operation (1920–2170 MHz) and the LTE2300/2500 operation (2300–2400/2500–2690 MHz), the near-field strengths of the electric and magnetic fields must be lower than 41 dBV/m and −9.4 dBA/m, respectively. In sum, the allowed maximum near-field emissions of the mobile phone above 960 MHz is 10 dB lower compared to those below 960 MHz. In addition, the allowed maximum near-field emissions of the GSM mobile phones should be 2.5 dB lower compared to other mobile phones.

To meet the HAC requirement, several promising internal antennas to be applied at the hinge position [2–5] or at the bottom edge [6] of the clamshell mobile phone for penta-band WWAN operation in the GSM850/900/1800/1900/UMTS bands have recently been reported. In these studies, as the acoustic output is located close to the top edge of the clamshell mobile phone, the distance between the acoustic output and the embedded antenna can be maximized. This arrangement is very helpful in achieving decreased near-field emission of the embedded antenna on the observation plane above the acoustic output.

Several techniques in decreasing the near-field emission of the embedded antennas have also been demonstrated [7–9]. These techniques include using an ultra-wideband (UWB) antenna [7], a wavetrap [8] along the side edge of the system circuit board of the mobile phone, and an LC filter at the hinge position of the clamshell mobile phone [9]. The latter two techniques [8, 9] decrease the excited surface currents around the acoustic output and in turn lead to decreased near-field emission on the observation plane above the acoustic output. For the UWB antennas, they generally have a low-Q property, which can lead to decreased near-field emission. However, from the reported HAC studies [2–9], promising designs of the bar-type mobile phone with the embedded antenna meeting the HAC requirement over the five WWAN operating bands of GSM850/900/1800/1900/UMTS and the three LTE operating bands of LTE700/2300/2500 are still not available. Note that by combining the LTE operation [10] with the WWAN operation [11], better mobile broadband and multimedia services can be provided for the mobile users. It is hence expected that the eight-band LTE/WWAN operation will soon become demanded in the modern mobile phones.

In this article, we present a promising HAC bar-type mobile phone design with its embedded antenna not only covering the eight-band LTE/WWAN operation but also meeting the HAC specification of ANSI C63.19-2007 over the eight operating bands. The antenna applied in the proposed HAC bar-type mobile phone is a coupled-fed on-board printed inverted-F antenna with a bypass radiating strip connected to the antenna's radiating portion to achieve a very wide upper band and a wide lower band. The two operating bands respectively cover the GSM1800/1900/UMTS/LTE2300/ 2500 operation (1710–2690 MHz) and the LTE700/GSM850/900 operation (698–960 MHz). Details of the operating principle of the applied antenna have been reported in [12]. It has been shown that by adding the bypass radiating strip, the variations in the input impedance of the antenna, especially for frequencies over the upper band, become much more smooth [see Fig. 3 in 12]. This behavior leads to widened bandwidths for the antenna studied in [12]. Also, it can be expected that a low-Q property [7] is obtained for the antenna, which is promising to result in decreased near-field emission of the mobile phone with the applied antenna.

In addition, because the antenna is disposed at the bottom edge of the system circuit board of the mobile phone and surrounded by an L-shaped ground plane (see Fig. 1), the excited surface currents on the main ground near the acoustic output located close to the top edge of the mobile phone casing can also be greatly decreased. The L-shaped ground plane arrangement can further lead to decreased near-field strengths of the emitted electric and magnetic fields on the observation plane above the acoustic output. The obtained near-field strengths of the proposed bar-type mobile phone are found to fall in category M3 or M4 of the HAC specification [1] for all the eight operating bands of the LTE/WWAN operation. Details of the HAC results of the studied antenna in the proposed mobile

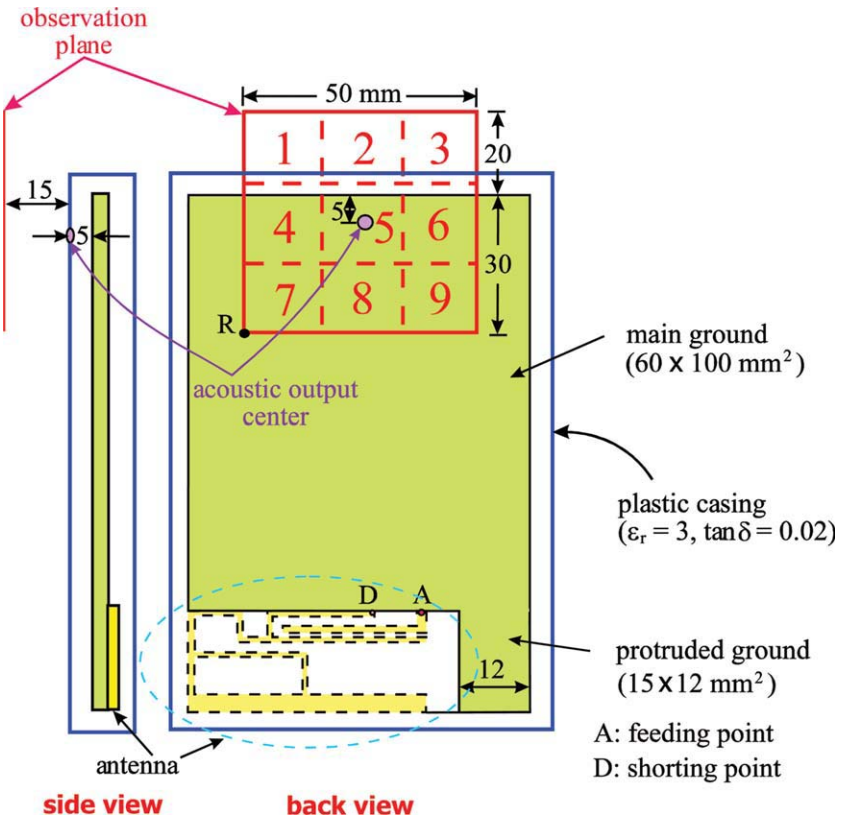

Figure 1 HAC simulation model of the bar-type mobile phone with an internal eight-band LTE/WWAN antenna surrounded by an L-shaped ground plane (the protruded ground and the main ground). [Color figure can be viewed in the online issue, which is available at wileyonlinelibrary.com]

phone are presented. Further, the near-field emissions for the case of the user's hand holding the proposed mobile phone are also studied.

2. THE PROPOSED LTE/WWAN MOBILE PHONE

Figure 1 shows the geometry of the proposed HAC bar-type mobile phone with the applied eight-band LTE/WWAN antenna. The antenna is on-board printed at the bottom edge of the system circuit board and surrounded by an L-shaped ground plane formed by a main ground and a protruded ground. The acoustic output center is located close to the top edge of the mobile phone casing, which is a plastic casing fabricated using a 1-mm-thick plastic material of relative permittivity 3.0 and conductivity 0.01 S/m. Owing to the presence of the plastic casing to simulate the practical mobile phone casing, the applied antenna does not require the top bent portion (see Fig. 1 in [12]) to widen the width of the antenna's radiating strip to shift downward the excited resonant modes and achieve enhanced bandwidths for the desired LTE/WWAN operation in the 698–960 and 1710–2690 MHz bands. In this case, the applied antenna in this study can be an all-printed structure disposed on the system circuit board of the mobile phone. This can make the antenna easy to fabricate and is especially attractive for applications in the slim or very slim mobile phones [13–16].

Design dimensions of the proposed LTE/WWAN antenna and the protruded ground connected to the main ground are shown in Figure 2. The antenna is disposed on a no-ground portion of size 15 × 48 mm^2 on the 0.8-mm-thick FR4 substrate (size 110 × 60 mm^2, relative permittivity 4.4, loss tangent 0.024) which is treated as the system circuit board of the mobile phone. On its back side, a main ground of 100 × 60 mm^2 and a protruded ground of 12 × 15 mm^2 is printed. Note that there is an 8-mm spacing between the protruded ground and the printed metal pattern of the antenna. This spacing is required to provide an isolation distance such that the coupling effects of the protruded ground affecting the antenna performances can be minimized and ignored.

The antenna is a coupled-fed printed inverted-F antenna, and its detailed operating principle has been studied in [12]. By using a coupling feed, the antenna can achieve a dual-resonance excitation [17–21] in the 900-MHz band, thereby leading to a wide lower band to cover the LTE700/GSM850/900 operation

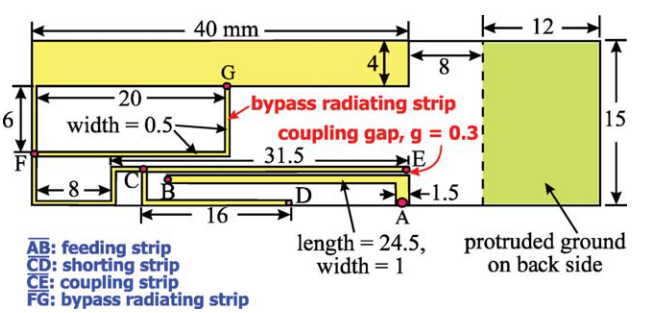

Figure 2 Dimensions of the proposed LTE/WWAN antenna and the protruded ground connected to the main ground. [Color figure can be viewed in the online issue, which is available at wileyonlinelibrary.com]

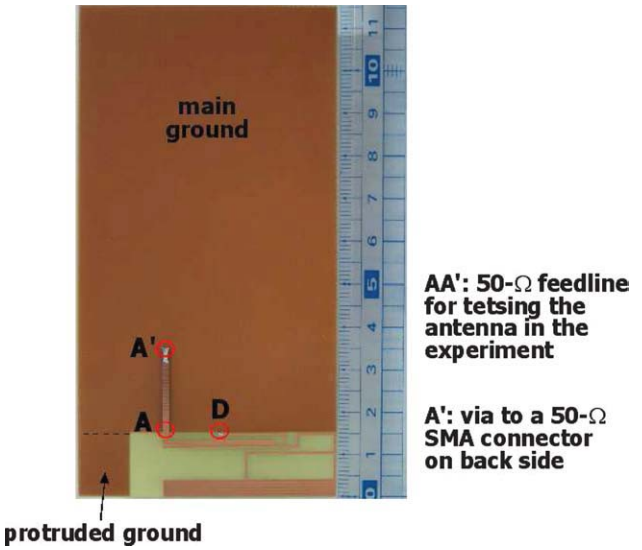

Figure 3 Photos of the fabricated antenna (plastic casing not shown in the photo). [Color figure can be viewed in the online issue, which is available at wileyonlinelibrary.com]

(698–960 MHz). By further applying a bypass radiating strip (section FG in Fig. 2), which provides a bypass for the excited surface currents on the antenna's radiating strip, more uniform excited surface current distributions can be expected. This feature can lead to slow variations in the antenna's input impedance over the operating bands, especially over the desired antenna's upper band (1710–2690 MHz). In this case, not only a wide operating band is achieved but also a low-Q property [7] is obtained for the antenna. This makes it very promising to obtain decreased near-field emission of the mobile phone with the applied antenna.

In addition, by using an L-shaped ground plane instead of a simple rectangular ground plane (no protruded ground in the proposed design), the excited surface currents on the main ground can be strongly affected such that much weaker surface current distributions in the vicinity of the acoustic output located at about the top edge of the mobile phone casing can be obtained. This can also lead to decreased near-field emission strengths obtained on the 50 × 50 mm^2 observation plane 15 mm centered above the acoustic output (ANSI C63.19-2007 [1]).

3. THE HAC RESULTS

To begin with the HAC study, the proposed antenna was fabricated and tested. Figure 3 shows the photo of the fabricated antenna. A comparison of the measured and simulated return loss is given in Figure 4. The simulated results are obtained using the SPEAG simulation software SEMCAD X version 14 [22]. The simulated results are in good agreement with the measured data. Results indicate that the proposed antenna can provide two wide operating bands to cover the eight-band LTE/WWAN operation (698–960/1710–2690 MHz). With good accuracy of the simulated results obtained, the HAC studies in the following are conducted using the SPEAG SEMCAD X.

Figure 5(a) shows the simulated near-field (E-field and H-field) distributions at 859, 1920, and 2350 MHz on the observation plane which is divided into nine equal-size cells. The HAC category rating is determined by excluding three consecutive cells [see the three crossed cells in each near-field distribution shown in Fig. 5(a)] along the boundary of the observation plane that have the strongest field strengths, and each category is 5 dB apart. The obtained maximum E-field and H-field strengths and the HAC categories at about the central frequencies of the eight operating bands are listed in a table in Figure 5(b).

The return loss given in the table indicates the impedance matching level at the testing frequency. In the study, the delivered power for the HAC study is 33 dBm (2 Watt continuous power) at 859 and 925 MHz for the GSM850/900 operation, and 30 dBm (1 Watt continuous power) at 1795 and 1920 MHz for the GSM1800/1900 operation, and 21 dBm (0.125 Watt continuous power) at 2045 MHz for the UMTS operation and at 740, 2350, and 2595 MHz for the LTE700/2300/2500 operation. The values of ΔE (ΔH) are the differences between the E-field (H-field) strength of the proposed design and the limit of the E-field (H-field) HAC M3 category. From the results, for the LTE and UMTS operating bands, the obtained near-field strengths are all rated in category M4, and the values of ΔE and ΔH are better than −17.0 dB. For the GSM operating bands, although larger delivered power is used for the HAC testing (30 and 33 dBm) and the HAC standard is also higher for the GSM operation, the obtained near-field strengths can still be rated in category M3. Hence, the obtained results show that all the E-field and H-field strengths are rated in at least category M3. That is, the proposed bar-type mobile phone with the applied LTE/WWAN antenna can be treated as a hearing aid-compatible wireless device.

To analyze the effect of the protruded ground on the obtained HAC results, Figures 6 and 7 show the simulated surface current distributions excited on the ground plane of the proposed design and the case without the protruded ground. It is clearly seen that with the presence of the protruded ground, the excited surface current distributions at around the portion of the main ground near the acoustic output center at the mobile phone casing become weaker. This behavior is mainly because the additional protruded ground is located close to the embedded internal antenna and can attract some strong excited surface currents that are originally on the main ground when the protruded ground is not present. This can, therefore, decrease the excited surface current

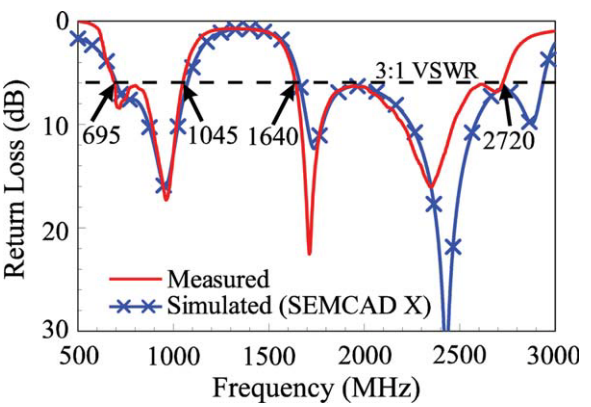

Figure 4 Measured and simulated return loss for the proposed antenna. [Color figure can be viewed in the online issue, which is available at wileyonlinelibrary.com]

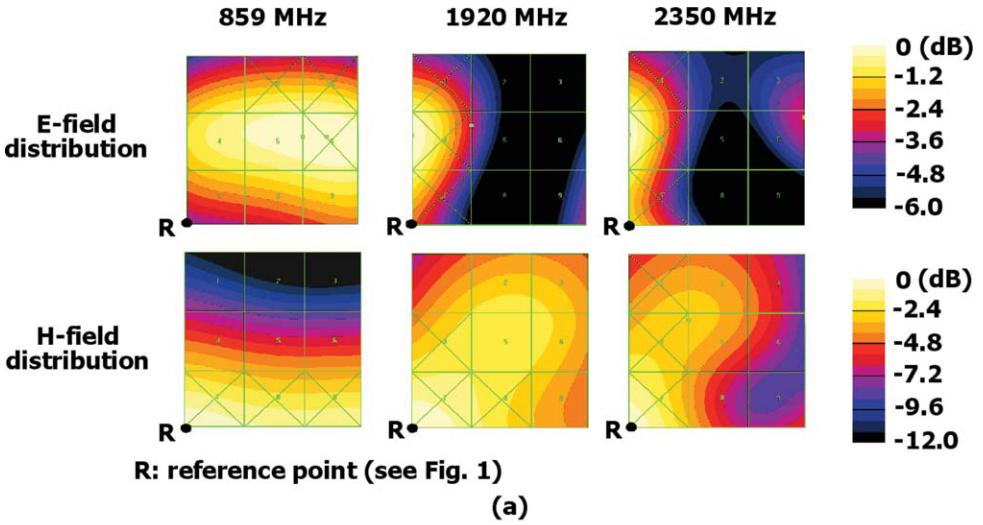

(a)

Operating band, Testing freq. (MHz)		LTE, 740	GSM, 859	GSM, 925	GSM, 1795	GSM, 1920	UMTS, 2045	LTE, 2350	LTE, 2595
E-field (V/m)	(dB)	33.8 (M4)	47.7 (M3)	47.6 (M3)	36.0 (M3)	33.3 (M3)	22.2 (M4)	21.4 (M4)	21.2 (M4)
	△E	-17.2	-0.8	-0.9	-2.5	-5.2	-18.8	-19.6	-19.8
H-field (A/m)	(dB)	-22.5 (M4)	-8.0 (M4)	-7.7 (M4)	-14.1 (M3)	-16.1 (M3)	-26.4 (M4)	-27.3 (M4)	-28.0 (M4)
	△H	-23.1	-6.1	-5.8	-2.2	-4.2	-17.0	-17.9	-18.6
Return loss	(dB)	7.4	9.4	14.1	9.3	6.4	6.7	16.2	9.3
Delivered power (W)	dBm	21	33	33	30	30	21	21	21

△E = E-field (proposed design) – limit of E-field HAC M3 category

△H = H-field (proposed design) – limit of H-field HAC M3 category

(b)

Figure 5 (a) Simulated near-field (E-field and H-field) distributions at 859, 1920, and 2350 MHz on the observation plane. (b) HAC E-field and H-field strengths and HAC categories at about the central frequencies of the eight operating bands. The return loss given in the table indicates the impedance matching level at the testing frequency. [Color figure can be viewed in the online issue, which is available at wileyonlinelibrary.com]

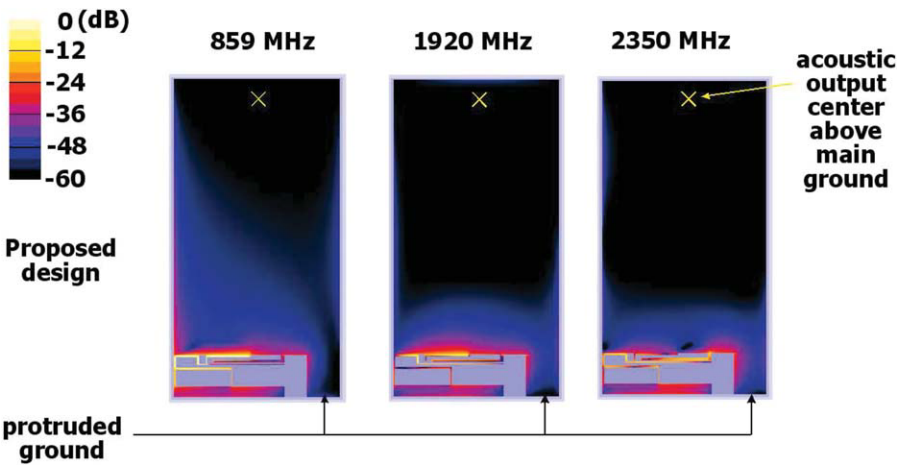

Figure 6 Simulated surface current distributions excited on the ground plane of the proposed design with an L-shaped ground plane. [Color figure can be viewed in the online issue, which is available at wileyonlinelibrary.com]

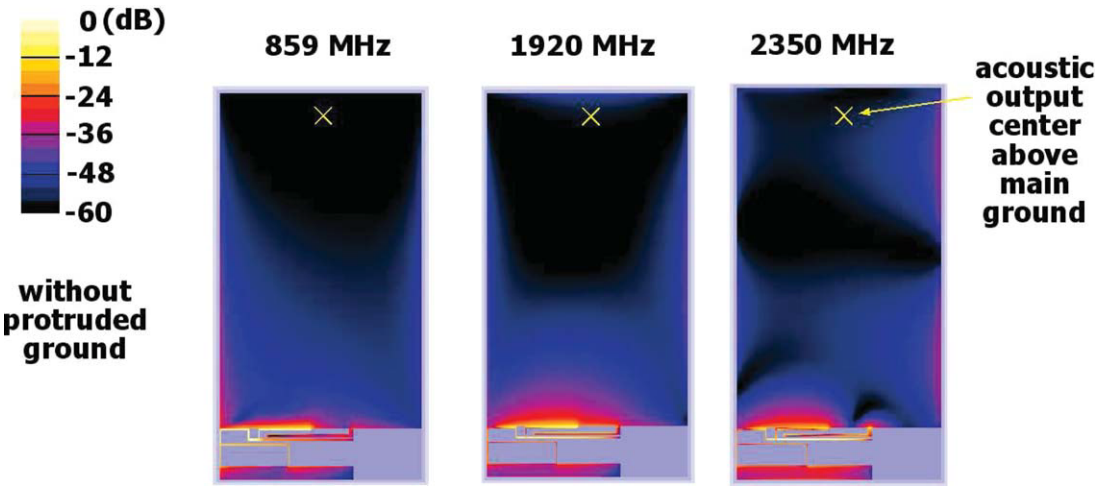

Figure 7 Simulated surface current distributions excited on the ground plane of the reference design with the main ground only (the protruded ground not present). [Color figure can be viewed in the online issue, which is available at wileyonlinelibrary.com]

distributions at around the opposite edge of the main ground. Hence, decreased near-field strengths of the E-field and H-field obtained on the HAC observation plane above the acoustic output center can be obtained. The decrease in the near-field strengths owing to the presence of the protruded ground is estimated to be about 2 dB in this study. The decreased

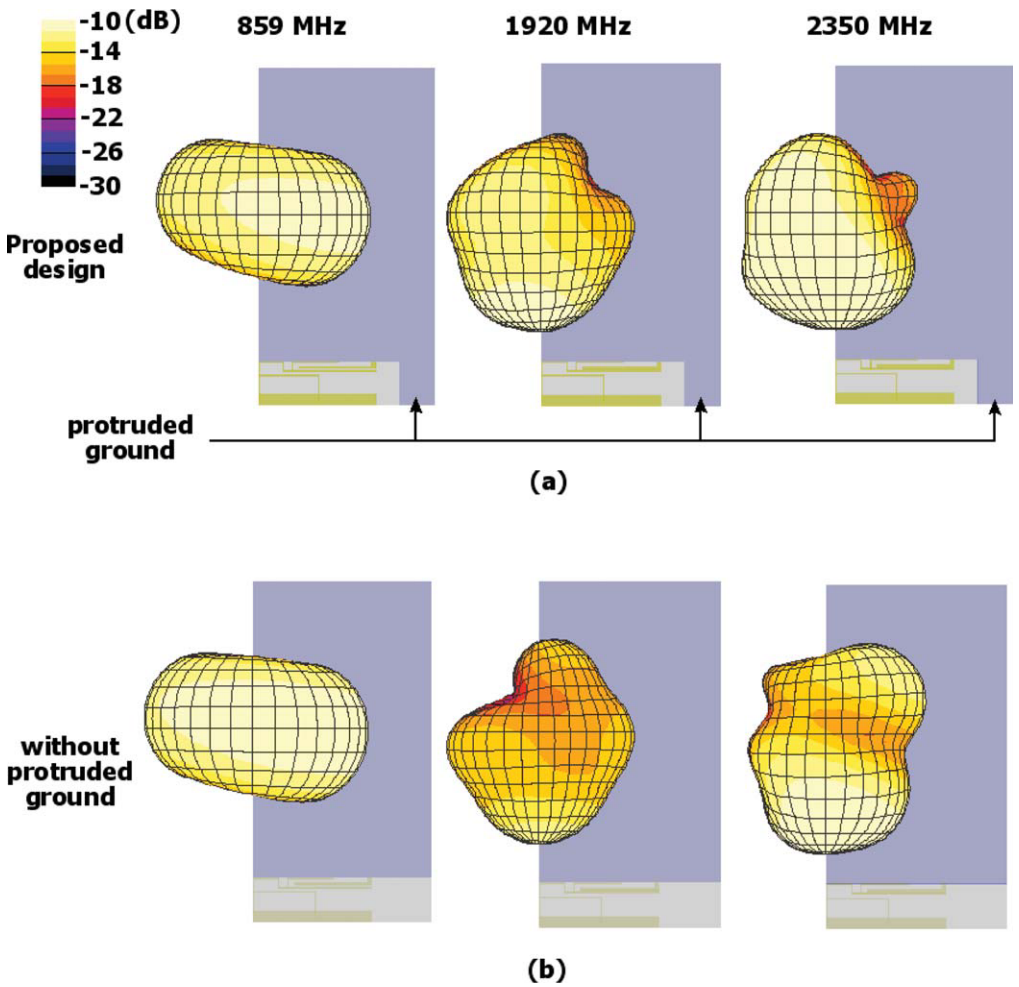

Figure 8 Simulated far-field total-power radiation patterns at 859, 1920, and 2350 MHz of (a) the proposed design with an L-shaped ground plane and (b) the reference design with the main ground only (the protruded ground not present). [Color figure can be viewed in the online issue, which is available at wileyonlinelibrary.com]

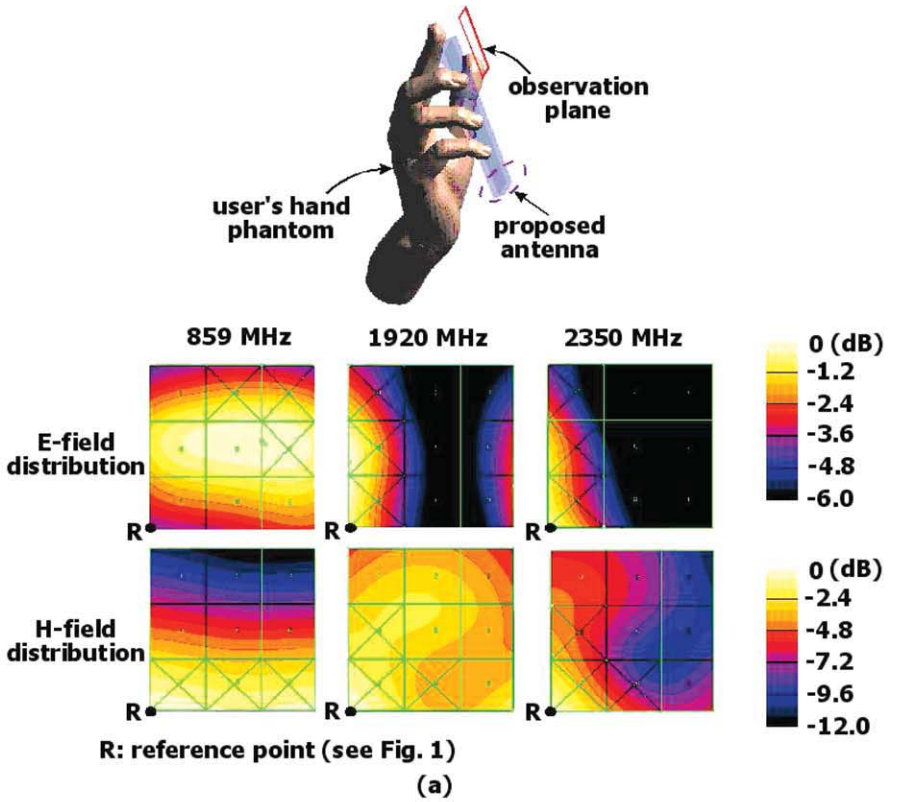

(a)

Operating band, Testing freq. (MHz)		LTE, 740	GSM, 859	GSM, 925	GSM, 1795	GSM, 1920	UMTS, 2045	LTE, 2350	LTE, 2595
E-field (V/m)	(dB)	32.9	46.4	46.4	33.1	31.1	20.8	20.8	19.6
	△E	-0.9	-1.3	-1.2	-2.9	-2.2	-1.4	-0.6	-1.6
H-field (A/m)	(dB)	-21.9	-7.9	-7.4	-16.1	-18.1	-28.2	-29.1	-32.1
	△H	+0.6	+0.1	+0.3	-2.0	-2.0	-1.8	-1.8	-4.1
Return loss	(dB)	9.7	12.3	18.2	7.9	4.9	5.2	14.7	9.9
	△RL	2.3	2.9	4.1	-1.4	-1.5	-1.5	-1.5	0.6
Delivered power (W)	dBm	21	33	33	30	30	21	21	21

△E = E(proposed design with hand presence) – E(proposed design)
△H = E(proposed design with hand presence) – E(proposed design)
△RL = RL(proposed design with hand presence) – RL(proposed design)

(b)

Figure 9 Near-field emission for the case with the presence of the user's hand. (a) Simulated near-field (E-field and H-field) distributions at 859, 1920, and 2350 MHz on the observation plane. (b) HAC E-field and H-field strengths at about the central frequencies of the eight operating bands. The return loss given in the table indicates the impedance matching level at the testing frequency. [Color figure can be viewed in the online issue, which is available at wileyonlinelibrary.com]

near-field strengths help the mobile phone meet the required HAC standard.

In addition to the improved HAC results, the protruded ground can also be used to accommodate the associated electronic components in the mobile phone. This helps achieve compact integration of the embedded internal antenna and the associated electronic components in the mobile phone. Also, owing to the protruded ground, which strongly modifies the excited surface currents on the main ground, the far-field radiation patterns in the azimuthal plane can become more omnidirectional as seen in Figure 8 in which the simulated radiation patterns at 859, 1920, and 2350 MHz of the proposed design and the case

without the protruded ground are plotted. From the comparison, it can be seen that at higher frequencies (1920 and 2350 MHz), the variations in the radiation patterns are smaller, especially in the azimuthal plane. With this radiation characteristic, the communication coverage of the mobile phone in all the ϕ direction of the azimuthal plane can be improved, which is attractive for practical mobile phone applications

4. NEAR-FIELD EMISSION WITH THE PRESENCE OF THE USER'S HAND

For the present, the HAC category rating is determined without the consideration of the user's hand. This does not conform to the practical conditions for the mobile users use their mobile phone. Hence, in this study, we also analyze the near-field emission for the case with the presence of the user's hand. The SEMCAD simulation model of the user's hand holding the mobile phone [23–28] is shown in Figure 9. The simulated near-field (E-field and H-field) distributions at 859, 1920, and 2350 MHz on the observation plane are shown in the figure. A table listing the maximum E-field and H-field strengths at about the central frequencies of the eight operating bands is also given in the figure. The return loss given in the table again indicates the impedance matching level at the testing frequency. Small variations on the return loss (ΔRL in the table) are seen. The E-field strengths at all the testing frequencies are seen to decrease with the presence of the user's hand. The decreases in the E-field strength (ΔE in the table) vary from -0.6 to -2.9 dB. This behavior is largely owing to the absorption of the E-field power by the user's hand. However, for the H-field, the strength variations (ΔH in the table) range from $+0.6$ to -4.1 dB. For lower frequencies, the presence of the user's hand causes an increase in the H-field strength, which is different from the observation of the E-field, whereas for higher frequencies, the variations in the H-field are similar to those for the E-field. The different behavior of the E-field and H-field at lower frequencies is largely related to the known near-field characteristic that the E-field and H-field are not closely related to each other in the near-field region. Hence, different results may occur for the E-field and H-field in the near-field region.

5. CONCLUSIONS

A promising HAC bar-type mobile phone for eight-band LTE/WWAN operation (698–960/1710–2690 MHz) has been proposed. The mobile phone uses an L-shaped ground plane formed by a main ground and a protruded ground and applies an on-board printed internal LTE/WWAN antenna which is expected to have a low-Q property to have decreased near-field emission. From the obtained results, the eight operating bands can all have an HAC category rating of at least M3 to be classified as an HAC mobile communication device, based on the ANSI C63.19-2007 specification. The physical explanations on achieving decreased HAC results have been described in the article. Effects of the user's hand holding the mobile phone have also been analyzed. The obtained results can provide useful information for considering the user's hand to be included in the HAC category rating.

REFERENCES

1. American National Standard for method of measurement of compatibility between wireless communication devices and hearing aids (ANSI C63.19–2007, revision ANSI C63.19–2006), American National Standards Institute, New York, 2007.
2. K.L. Wong and M.F. Tu, Hearing aid-compatible internal penta-band antenna for clamshell mobile phone, Microwave Opt Technol Lett 51 (2009), 1408–1413.
3. K.L. Wong and S.Y. Tu, Ultra-wideband coupled-fed loop antenna for penta-band folder-type mobile phone, Microwave Opt Technol Lett 50 (2008), 2706–2712.
4. W.Y. Li and K.L. Wong, Small-size WWAN loop chip antenna for clamshell mobile phone with hearing-aid compatibility, Microwave Opt Technol Lett 51 (2009), 2327–2335.
5. W.Y. Chen and K.L. Wong, Wideband coupled-fed PIFA for HAC penta-band clamshell mobile phone, Microwave Opt Technol Lett 51 (2009), 2369–2374.
6. W.Y. Li and K.L. Wong, Internal wireless wide area network clamshell mobile phone antenna with reduced ground plane effects, Microwave Opt Technol Lett 52 (2010), 922–930.
7. T. Yang, W.A. Davis, W.L. Stutzman, and M.C. Huynh, Cellular-phone and hearing-aid interaction: An antenna solution, IEEE Antennas Propag Mag 50 (2008), 51–65.
8. J. Holopainen, J. Ilvonen, O. Kivekas, R. Valkonen, C. Icheln, and P. Vainikainen, Near-field control of handset antennas based on inverted-top wavetraps: Focus on hearing-aid compatibility, IEEE Antennas Wireless Propag Lett 8 (2009), 592–595.
9. A. Zhao, J. Ollikainen, J. Thaysen, and T. Bodvarsson, A novel approach to reduce the near field electromagnetic scattering for designing HAC compatible mobile phones, Microwave Opt Technol Lett 51 (2010), 709–715.
10. S. Sesia, I. Toufik, and M. Baker (Eds.), LTE, The UMTS long term evolution: From theory to practice, Wiley, New York, 2009.
11. K.L. Wong, Planar antennas for wireless communications, Wiley, New York, 2003.
12. S.C. Chen and K.L. Wong, Bandwidth enhancement of coupled-fed on-board printed PIFA using bypass radiating strip for eight-band LTE/GSM/UMTS slim mobile phone, Microwave Opt Technol Lett 52 (2010), 2059–2065.
13. C.H. Chang and K.L. Wong, Printed $\lambda/8$-PIFA for penta-band WWAN operation in the mobile phone, IEEE Trans Antennas Propagat 57 (2009), 1373–1381.
14. Y.W. Chi and K.L. Wong, Quarter-wavelength printed loop antenna with an internal printed matching circuit for GSM/DCS/PCS/UMTS operation in the mobile phone, IEEE Trans Antennas Propag 57 (2009), 2541–2547.
15. W.Y. Chen and K.L. Wong, Small-size coupled-fed shorted T-monopole for internal WWAN antenna in the slim mobile phone, Microwave Opt Technol Lett 52 (2010), 257–262.
16. K.L. Wong and S.C. Chen, Printed single-strip monopole using a chip inductor for penta-band WWAN operation in the mobile phone, IEEE Trans Antennas Propag 58 (2010), 1011–1014.
17. K.L. Wong and C.H. Huang, Bandwidth-enhanced internal PIFA with a coupling feed for quad-band operation in the mobile phone, Microwave Opt Technol Lett 50 (2008), 683–687.
18. C.H. Chang and K.L. Wong, Internal coupled-fed shorted monopole antenna for GSM850/900/1800/1900/UMTS operation in the laptop computer, IEEE Trans Antennas Propag 56 (2008), 3600–3604.
19. K.L. Wong and C.H. Huang, Printed PIFA with a coplanar coupling feed for penta-band operation in the mobile phone, Microwave Opt Technol Lett 50 (2008), 3181–3186.
20. C.H. Chang, K.L. Wong, and J.S. Row, Coupled-fed small-size PIFA for penta-band folder-type mobile phone application, Microwave Opt Technol Lett 51 (2009), 18–23.
21. K.L. Wong and S.J. Liao, Uniplanar coupled-fed printed PIFA for WWAN operation in the laptop computer, Microwave Opt Technol Lett 51(2009), 549–554.
22. Available at http://www.semcad.com, SPEAG SEMCAD, Schmid & Partner Engineering AG.
23. C.M. Su, C.H. Wu, K.L. Wong, S.H. Yeh, and C.L. Tang, User's hand effects on EMC internal GSM/DCS dual-band mobile phone antenna, Microwave Opt Technol Lett 48 (2006), 1563–1569.

24. C.I. Lin, K.L. Wong, S.H. Yeh, and C.L. Tang, Study of an L-shaped EMC chip antenna for UMTS operation in a PDA phone with the user's hand, Microwave Opt Technol Lett 48 (2006), 1746–1749.
25. C.I. Lin and K.L. Wong, Printed monopole slot antenna for internal multiband mobile phone antenna, IEEE Trans Antennas Propag 55 (2007), 3690–3697.
26. C.I. Lin and K.L. Wong, Internal meandered loop antenna for GSM/DCS/PCS multiband operation in a mobile phone with the user's hand, Microwave Opt Technol Lett 49 (2007), 759–765.
27. C.T. Lee and K.L. Wong, Study of a uniplanar printed internal WWAN laptop computer antenna including user's hand effects, Microwave Opt Technol Lett 51 (2009), 2341–2346.
28. C.H. Li, E. Ofli, N. Chavannes, and N. Kuster, Effects of hand phantom on mobile phone antenna performance, IEEE Trans Antennas Propag 57 (2009), 2763–2770.

A NOVEL WIDEBAND WILKINSON DIVIDER USING PARALLEL BRANCH LINES

Peng Wu,[1] Yong Zhang,[1] and Qin Zhang[2]
[1] EHF Key Laboratory of Fundamental Science, School of Electronic Engineering, University of Electronic Science and Technology of China (UESTC), Chengdu, 611731, China; Corresponding author: pengwu2009@hotmail.com
[2] School of Microelectronics and Solid-State Electronics, UESTC, Chengdu, 610054, China

Received 25 June 2010

ABSTRACT: *A novel wideband branch line Wilkinson divider is proposed. Branch lines are introduced to replace multiple resistors used in the multistage Wilkinson divider to increase the bandwidth of a single-stage Wilkinson divider. To demonstrate its performance, a modified single-stage Wilkinson divider with four branch lines has been fabricated and measured. Results show that the measured input return loss, output return loss, and isolation are better than 12.4, 11.6, and 15 dB, respectively, across a 72% bandwidth from 18.8 to 40 GHz.* © 2011 Wiley Periodicals, Inc. Microwave Opt Technol Lett 53:781–783, 2011; View this article online at wileyonlinelibrary.com. DOI 10.1002/mop.25833

Key words: *branch-line; wideband; Wilkinson divider*

1. INTRODUCTION

The Wilkinson power divider is one of the most widely used passive elements, which allows microwave signals to split equally or unequally. A simplest Wilkinson divider is shown in Figure 1(a). It is a single-stage component with 50 Ω input and output ports, two 70.7 Ω quarter-wavelength transformers and a 100 Ω resistor bridged between the two output ports to provide isolation and matching. Its disadvantage is the limited bandwidth. Due to the rapid growth of wireless communications, wideband components are tremendously required, so does the wideband Wilkinson divider. Therefore, the investigation of the wideband Wilkinson divider is significant at this time. For this purpose, manly wideband power dividers [1–6] have been developed so far. But a few of them introduce the millimeter-wave wideband Wilkinson divider. Normally, a multistage Wilkinson divider has an improved operation bandwidth over a standard single-stage Wilkinson divider [1–4]. According to the characteristics of the millimeter-wave Wilkinson divider, as the operating frequency increases, the impact of parasitic parameters of the chip resistor will become tremendous. If the number of the chip resistors increases, the performance of the millimeter-wave Wilkinson divider will be deteriorated. In this article, a novel millimeter-wave wideband Wilkinson divider using parallel branch lines is presented to overcome the influence of the multiple resistors and increase the bandwidth of a single-stage Wilkinson divider effectively.

2. DIVIDER DESIGN

A general circuit of the multistage Wilkinson divider is shown in Figure 1(b). It contains N pairs of equal-length transmission lines and N bridging resistors distributed from the input port to two output ports [2]. It is most easily analyzed by the method of even- and odd-mode excitations [7]. It is well known that as the number of transmission line sections and resistors is increased, the bandwidth of a Wilkinson divider is improved effectually. To attain broadband isolation, the resistors of the multistage Wilkinson divider provide multiple transmission paths of electromagnetism wave, such as path 1, path 2, path N, and so on, as shown in Figure 1(b). In [8], a modified Wilkinson divider for suppressing the *n*th-harmonic output is presented by adding stub transmission lines between the resistor and each output port. We can image that the multiple resistors in Figure 1(b) can be replaced by branch lines to increase the bandwidth of a single-stage Wilkinson divider. Then, a novel wideband Wilkinson divider is proposed. To demonstrate its modified performance, a broadband Wilkinson divider with four branch lines is designed using only one resistor in Figure 2(a). It is modeled by using the Ansoft HFSS and fabricated on the Rogers RT/duroid 5880 dielectric substrate with a relative dielectric constant of 2.2 and a thickness of 0.254 mm. A 0402 chip resistor of 100 Ω is used in our design. The original dimensions of the divider are determined by the same way used in multistage Wilkinson divider design. In addition, the multiple resistors are replaced by branch lines of the same characteristic impedance. To minimize the complexity of the simulated model, its two main output lines are designed with the same width of 0.76 mm, and all the

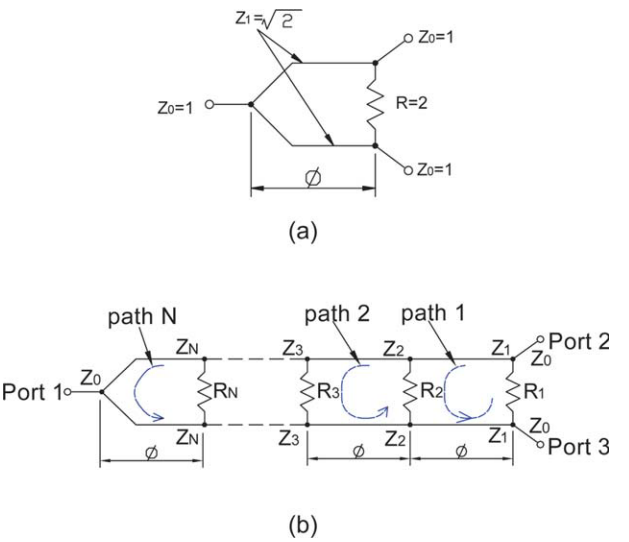

Figure 1 General circuits of Wilkinson divider: (a) Simplest Wilkinson divider and (b) Multistage Wilkinson divider. [Color figure can be viewed in the online issue, which is available at wileyonlinelibrary.com]